HiSST: 3rd International Conference on High-Speed Vehicle Science Technology

14 -19 April 2024, Busan, Korea

The development of a design program for a high-speed counter-flow air precooler

Zhang X, Lu Y [1], Fan XJ

Abstract

The precooler is the core component of the precooled air-breathing combined engine, which is used to cool the incoming high-temperature air in a short time. A gas-solid-liquid coupled heat transfer program is developed to evaluate the flow heat transfer performance of a high-speed counter-flow air precooler. The program uses two methods to calculate the heat conduction of the solid. One is the "Node Current Method", which is suitable for rapid evaluation of the performance of the precooler. The other is the "Fenics Finite Element Platform", which is suitable for the performance evaluation of the precooler with complex structural shapes and stress analysis. The program can be used to evaluate the cooling performance of various coolants such as hydrogen, methane, ammonia and kerosene. The fuel cracking mechanism has been added to the program when calculating kerosene. The calculation results of two methods have been compare using hydrogen and methane as coolants. The relative error of calculated air outlet temperature is less than 1.1%. Kerosene with cracking mechanism has also been calculated when it is used to cool the 1800 K incoming air. To sum up, the high-speed counter-flow air precooler is suitable for the cooling of the air from Ma 2.5 to Ma 6.5, which corresponds to the temperature of 486 K to 1800 K. The program evaluates the heat transfer performance of the precooler well and is suitable for the evaluation of different forms of counter-flow air precooler.

Keywords: *Air precooler, Node Current Method, Fenics Finite Element Platform, counter-flow, Cracking*

1. Introduction

The wide-speed range engine is the core component of the propulsion system of future space vehicles. To meet the demand for long-time working capability, researchers have proposed various concepts of variable-cycle and combined-cycle engines[1-2]. Among them, the turbo-based combined cycle (TBCC) engine, with the advantages of horizontal take-off and landing, lower oxidizer loading, and higher reliability, has become the focus of hypersonic propulsion research in recent years[3-4]. However, scramjets cannot provide sufficient thrust below Mach 4, and the existing turbine engine has insufficient thrust above Mach 2.5 due to the limited temperature of the compressor outlet, leading to the intractable thrust gap problem. To solve this problem, the researchers propose an air precooling technology route that uses the on-board coolant to cool the air, thereby increasing the maximum operating Mach number of the turbine mode.

The high-efficiency lightweight heat exchanger is the common core component of all fuel precooled engines. The heat exchanger of precooled combined engines must have a high volume and mass power density. If the volume and mass of the heat exchanger is too large, the engine will lose its practical value. Therefore, the heat exchanger of the precooled combined engine must generally use micro-channel heat exchange surface to greatly improve the compactness of the heat exchanger[5]. Taking the configuration of precooler of ATREX and SABRE cycle as an example. The precooler of ATREX is a typical shell-and-tube heat exchanger[6]. The precooler uses liquid hydrogen fuel directly as the cooling medium, and the air flows through the tube to complete the heat exchange with the hydrogen fuel. After many tests, in addition to increasing the air-side pressure drop, the micro-channel precooler has advantages in terms of heat transfer performance, volume, weight and compactness. The SABRE engine

1 *Institute of Mechanics, Chinese Academy of Sciences. Beijing, China. luyang@imech.ac.cn*

precooler consists of tens of thousands of 0.88 mm OD, 0.04 mm wall thickness round tubes arranged radially in a spiral[7]. The tubes are arranged in a forked row. The helium working fluid flows along the tube from the inside to the outside, while the air flows radially from the outside to the inside, forming an equivalent countercurrent heat exchanger.

For a counter-flow tube-fin air precooler, a design program is developed in the paper. Two methods are used to calculate the differential equation for the thermal conductivity of the precooler wall, which can be used in various configurations. And the program couples REFPROP and SUPERTRAPP subroutines developed by NIST to calculate different types of coolants. The program is instructive for precooler design and its performance prediction.

2. Modeling method

2.1. Heat transfer analysis of air and coolant

To calculate the flow and heat transfer in the hot and cold fluid channel, the following assumptions need to be made:

(1) Since the hot and cold fluid channel as a whole is an elongated structure, the geometry of the cross section does not usually change drastically, so the flow and heat transfer of the hot and cold fluids in the channel is simplified to a one-dimensional problem in the calculation process, and there is basically no change in the physical properties of the hot and cold fluids in the radial direction;

(2) The influence of the thermal boundary layer in the hot and cold fluid channel is not considered;

(3) The normal temperature gradient of the channel wall is much larger than the temperature gradient in the flow direction, if a sufficiently large number of cooling structure cross sections are divided along the flow direction, the heat conduction between adjacent cross sections can be basically ignored, and the three-dimensional steady-state heat conduction problem of the whole precooler structure is transformed into a number of mutually independent two-dimensional steady-state heat conduction problems to be solved, which can effectively reduce the amount of computation;

(4) The flow of hot and cold fluids, convective heat transfer and other processes have reached steady state.

The schematic diagram of a structural unit of the precooler channel is shown in Figure 1, surrounded by two adjacent sections.

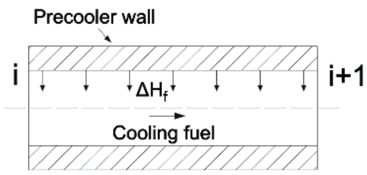

Fig 1. Schematic diagram of the precooler channel structure unit

The flow heat transfer characteristics of the fluid between two adjacent cross sections are related by the continuity equation, the energy equation and the momentum equation, and the forms of the three equations are shown as follows.

The continuity equation

$$\dot{m}_i = \rho_i u_i A_i = \rho_{i+1} u_{i+1} A_{i+1} \tag{1}$$

Where ρ is the fluid density, u is the fluid velocity, and A is the cross section area of the channel.

The energy equation

$$\dot{m}_i \left(H_i + 1/2 \cdot u_i^2 \right) = \dot{m}_{i+1} \left(H_{i+1} + 1/2 \cdot u_{i+1}^2 \right) + \Delta H_i \tag{2}$$

Where

$$\Delta H_i = 0.5 \cdot \left(q_i + q_{i+1} \right) S_i \cdot dx \tag{3}$$

$$q_i = h_i \cdot \left| T_i - T_{w,i} \right| \tag{4}$$

$$h_i = \left(Nu_i \cdot \lambda_i\right) / D_h \tag{5}$$

$$Nu = \begin{cases} 4.089, \ Re \le 2300 \\ 4.089 + \left(Nu_{G|Re-5000} - 4.089\right) / \left(5000 - 2300\right), \ 2300 < Re < 5000 \\ \left(f/2 \cdot \left(Re - 1000\right) Pr\right) / \left(1 + 12.7\left(Pr^{2/3} - 1\right)\sqrt{f/2}\right), \ Re \ge 5000 \end{cases} \tag{6}$$

$$f = \left(1.8 logRe - 1.5\right)^{-2} / 4 \tag{7}$$

Where q is the heat flux at the cross section, S is the circumference of the cross section, h is the heat transfer coefficient of the fluid at the cross section, λ is the thermal conductivity of the fluid, and D_h is the hydraulic diameter of the channel.

The momentum equation

$$\dot{m}_i u_i + p_i A_i + \int_i^{i+1} p dA = \dot{m}_{i+1} u_{i+1} + p_{i+1} A_{i+1} + \int_i^{i+1} \tau_w dA \tag{8}$$

$$\tau_w = f/2 \cdot \rho u^2 \tag{9}$$

Where τ_w is the frictional stress on the channel wall and μ is the dynamic viscosity of the fluid.

2.2. Calculation of wall heat conduction

Two methods are used to calculate the differential equation for the thermal conductivity of the precooler wall, the "Node Current Method"[8] and the "Fenics Finite Element Platform"[9]. Computational domain meshing for two methods is shown in Fig.2.

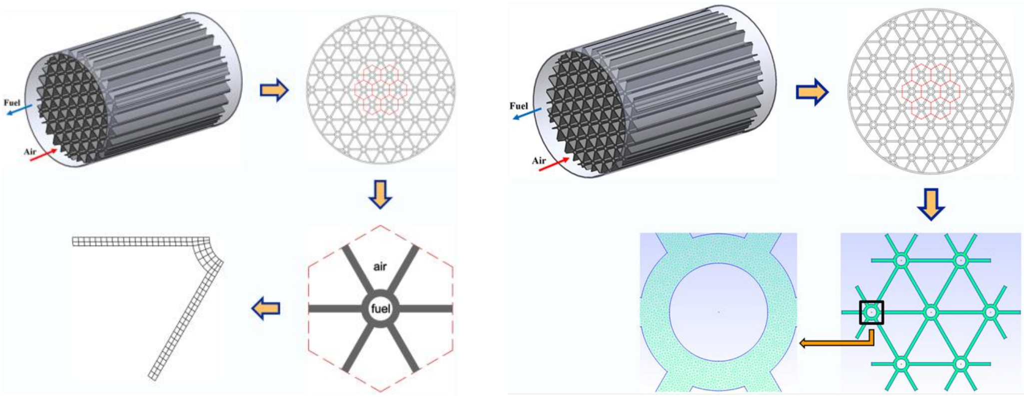

(a) Node Current Method (b) Fenics Finite Element Platform

Fig 2. Mesh for cross section

The calculation process of the "Node Current Method" is as follows.

The two-dimensional differential equations of thermal conductivity in rectangular and polar coordinates are shown as follows.

Rectangular coordinate system

$$\frac{1}{\partial x}\left(k\frac{\partial T}{\partial x}\right) + \frac{\partial}{\partial y}\left(k\frac{\partial T}{\partial y}\right) + s = 0 \tag{10}$$

Polar coordinate system

$$\frac{1}{r}\frac{1}{\partial r}\left(rk\frac{\partial T}{\partial r}\right) + \frac{1}{r}\frac{\partial}{\partial \theta}\left(\frac{k}{r}\frac{\partial T}{\partial \theta}\right) + s = 0 \tag{11}$$

Where s is internal heat source.

The two-dimensional universal discrete equation without internal heat source at nodes (i, j) is

$$\frac{T_{i+1,j}-T_{i,j}}{R_1}+\frac{T_{i,j+1}-T_{i,j}}{R_2}+\frac{T_{i-1,j}-T_{i,j}}{R_3}+\frac{T_{i,j-1}-T_{i,j}}{R_4}=0 \tag{12}$$

The temperature at node (i, j) is

$$T_{i,j}=\left(\frac{T_{i+1,j}}{R_1}+\frac{T_{i,j+1}}{R_2}+\frac{T_{i-1,j}}{R_3}+\frac{T_{i,j-1}}{R_4}\right)\Big/\left(\frac{1}{R_1}+\frac{1}{R_2}+\frac{1}{R_3}+\frac{1}{R_4}\right) \tag{13}$$

The thermal resistance calculation formula is

$$\begin{cases} R_1=\dfrac{\Delta X_{i+1,j}}{\Delta Y_{i+1,j}}\dfrac{1}{2}\left(\dfrac{1}{k_{i,j}}+\dfrac{1}{k_{i+1,j}}\right) \\ R_2=\dfrac{\Delta Y_{i,j+1}}{\Delta X_{i,j+1}}\dfrac{1}{2}\left(\dfrac{1}{k_{i,j}}+\dfrac{1}{k_{i,j+1}}\right) \\ R_3=\dfrac{\Delta X_{i-1,j}}{\Delta Y_{i-1,j}}\dfrac{1}{2}\left(\dfrac{1}{k_{i,j}}+\dfrac{1}{k_{i-1,j}}\right) \\ R_4=\dfrac{\Delta Y_{i,j-1}}{\Delta X_{i,j-1}}\dfrac{1}{2}\left(\dfrac{1}{k_{i,j}}+\dfrac{1}{k_{i,j-1}}\right) \end{cases} \tag{14}$$

The overrelaxation iterative method is used to calculate the two-dimensional steady state thermal conductivity discrete equation

$$T_{i,j}^{n+1}=T_{i,j}^{n}+\Omega\left(T_{i,j}-T_{i,j}^{n}\right) \tag{15}$$

The superscript n represents the number of iterations, and Ω is the relaxation factor with a value of 1.5.

The calculation process of the " Fenics Finite Element Platform" is as follows.

Fenics is an open source computing platform for solving partial differential equations by finite element method based on python, which converts thermal conductivity differential equations into variational form

For the following thermal conductivity differential equation containing three types of boundary conditions (s represents the internal heat source)

$$\begin{aligned} &\nabla\cdot\left(k\nabla T\right)=-s,\ \text{in}\ \Omega \\ &T=T_D^i,\ \text{on}\ \Gamma_D^i,\ i=0,1\ldots \\ &-k\frac{\partial T}{\partial n}=q_i,\ \text{on}\ \Gamma_N^i,\ i=0,1\ldots \\ &-k\frac{\partial T}{\partial n}=h_i\cdot\left(T-T_{0,i}\right),\ \text{on}\ \Gamma_R^i,\ i=0,1\ldots \end{aligned} \tag{16}$$

In the above equation, Γ_D, Γ_N and Γ_R are the first, second and third kinds of boundaries of the thermal conductivity differential equation, and the wall temperature, heat flux, convective heat transfer coefficient and fluid temperature at the boundary are given, respectively.

Both sides of the thermal conductivity differential equation are multiplied by the test function v and integrated in the global Ω

$$\int_\Omega \nabla\cdot\left(k\nabla T\right)v dx=-\int_\Omega svdx \tag{17}$$

Test functions and trial functions are defined as

$$\hat{V}=\left\{v\in H^1\left(\Omega\right):v=0\ \text{on}\ \Gamma_D^i\right\} \tag{18}$$

$$V=\left\{T\in H^1\left(\Omega\right):T=T_D^i\ \text{on}\ \Gamma_D^i\right\} \tag{19}$$

The H1(Ω) function space represents that the test and trial functions and their first derivatives are square-integrable in the global Ω. For the test function v, it is 0 on the first kind of boundary conditions of the thermal conductivity differential equation.

Then the term in the integral symbol on the left of equation (17) is integrated by parts, and the result is as follows

$$\nabla\cdot\left(k\nabla T\right)v=\nabla\cdot\left(k\nabla Tv\right)-k\nabla T\cdot\nabla v \tag{20}$$

The first term to the right of equation (20) is transformed into a line integral on the boundary of the differential equation by using Gauss's theorem.

$$\int_{\Omega}\nabla\cdot\left(k\nabla Tv\right)dx=\int_{\partial\Omega}n\cdot\left(k\nabla Tv\right)ds=\int_{\partial\Omega}k\frac{\partial T}{\partial n}vds \tag{21}$$

After sorting out the above equations, the following equations are obtained

$$-\int_{\Omega}k\nabla T\cdot\nabla vdx+\int_{\partial\Omega}k\frac{\partial T}{\partial n}vds+\int_{\Omega}svdx=0 \tag{22}$$

$$\int_{\Omega}k\nabla T\cdot\nabla vdx+\sum_i\int_{\Gamma_N^i}q_ivds+\sum_i\int_{\Gamma_R^i}h_i\cdot\left(T-T_{0,i}\right)vds-\int_{\Omega}svdx=0 \tag{23}$$

Since the test function v is equal to 0 on the first kind of boundary, the integral value on the first kind of boundary in equation (23) is 0.

The bivariate integral terms of test function T and test function v, and the univariate integral terms of test function v are sorted out, respectively

$$a\left(T,v\right)=\int_{\Omega}k\nabla T\cdot\nabla vdx+\sum_i\int_{\Gamma_R^i}h_iTvds \tag{24}$$

$$L\left(v\right)=\int_{\Omega}svdx-\sum_i\int_{\Gamma_N^i}q_ivds+\sum_i\int_{\Gamma_R^i}h_iT_{0,i}vds \tag{25}$$

The thermal conductivity differential equation is converted into the standard form of the following variational problem. That is to seek trial function T∈V, satisfied

$$a\left(T,v\right)=L\left(v\right)\qquad\forall v\in\hat{V} \tag{26}$$

Fenics solved the variational problem by finite element method.

3. Numerical model validation

Due to the lack of reported supercritical heat transfer experimental data for precooler, in this paper, we choose the experimental data on single-tube heating from the literature [10] to validate the results of the heat transfer calculations. The comparison results are shown in Fig.3. As shown, the calculated results agree well with the experiment results, with errors within 5%.

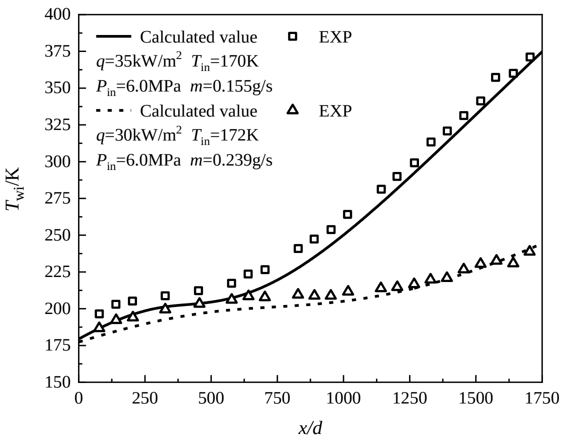

Fig 3. The comparison of the calculated inner wall temperature and the experimental values

4. Results and discussion

This section compares the difference between the calculation results of two wall temperature iteration methods, "Node Current Method" and "Fenics Finite Element Platform", using hydrogen and methane as coolants respectively. Fig.4 and Fig.5 show the comparison of axial and radial temperature distributions respectively. As shown in Fig.4, the fluid temperature curves have a gentle slope at the critical temperature, and correspondingly the mean wall temperature curves have a minimum value. This is because the coolant's specific heat capacity at constant pressure reaches its maximum at the critical temperature. As shown in Fig.5,the radial distribution of the wall temperature shows a tendency to be highest in the centre of the fin and lowest in the wall of the cooling channel. The relative error of calculated air outlet temperatures is less than 1.1% for two methods. The accuracy of the program calculation results can also be verified by the comparison of the two methods.

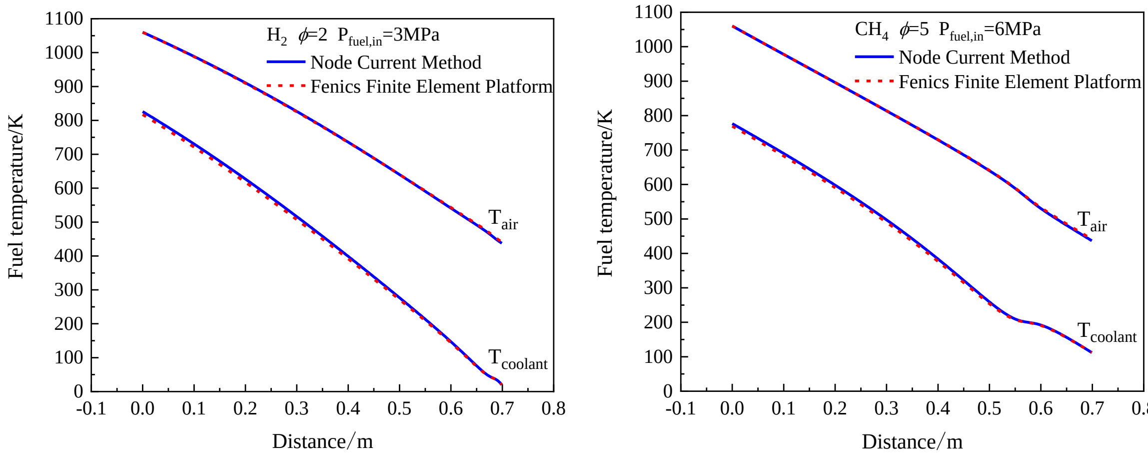

(a) Fuel temperature

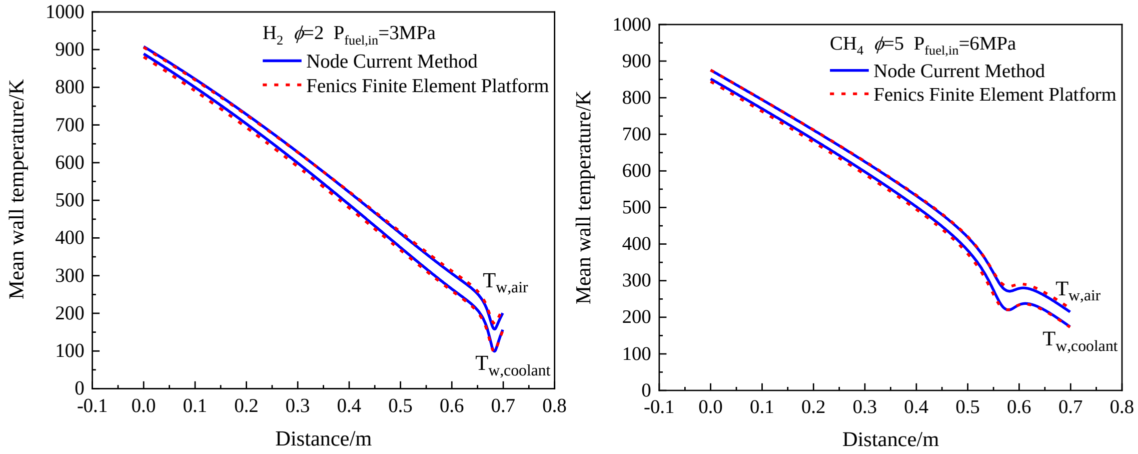

(b) Mean wall temperature

Fig 4. Comparison of axial temperature distributions

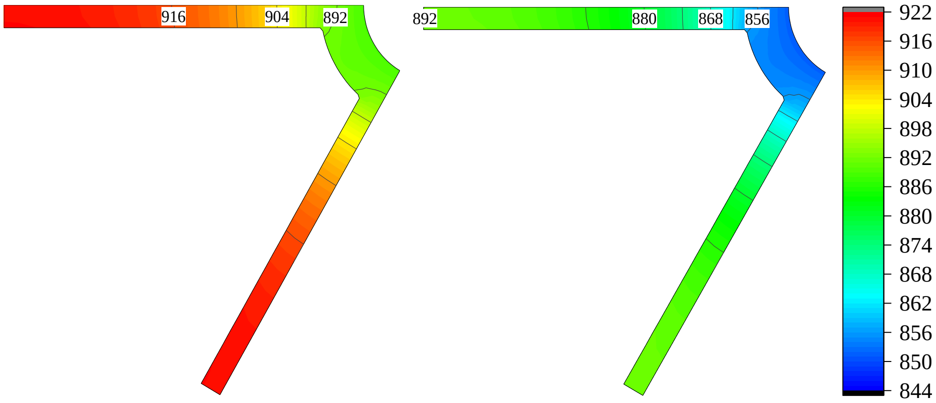

(a) Node Current Method

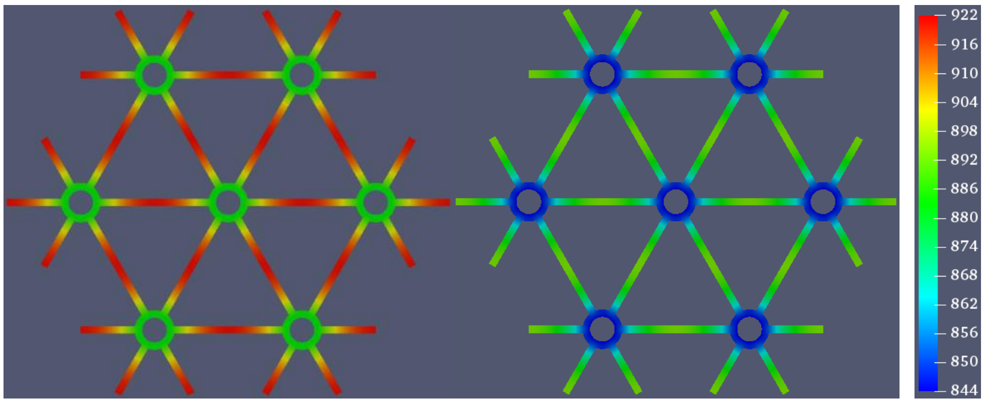

H_2 CH_4

(b) Fenics Finite Element Platform

Fig 5. Comparison of radial temperature distributions (x=0)

In addition, the performance of the precooler is also calculated when hydrocarbon fuels are used as the coolant. The program uses the Supertrapp software developed by NIST to obtain the physical properties of hydrocarbon fuels. Based on the experimental data of the thermal-physical properties of RP-3 kerosene, a 5-component surrogate model is obtained using the Matlab optimisation toolbox. As shown in Fig.6 and Fig.7, kerosene with cracking mechanism is calculated when it is used to cool the 1800 K incoming air, and the total pressure of incoming air is 150 kPa. As shown in Fig.6, at a kerosene flow rate of 240 g/s, 1800 K incoming air at a flow rate of 0.5 kg/s can be cooled to 1177 K at a distance of 350 mm, the kerosene outlet temperature is 833 K and the maximum structure temperature is 1100 K. As shown in Fig.7, at a kerosene flow rate of 1.875 kg/s, 1800 K incoming air at a flow rate of 0.5 kg/s can be cooled to 1208 K at a distance of 170 mm, the kerosene outlet temperature is 425 K and the maximum structure temperature is 813 K.

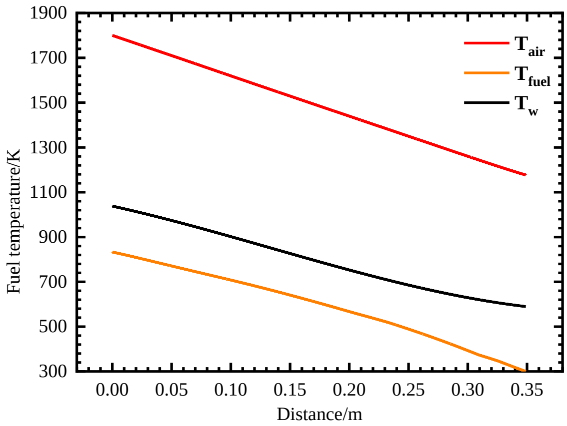

Fig 6. The calculated results of kerosene with cracking mechanism ($P_{air,in}$=150 kPa)

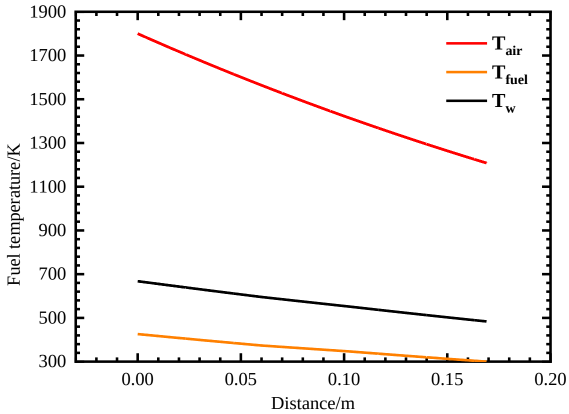

Fig 7. The calculated results of kerosene with cracking mechanism ($P_{air,in}$=150 kPa, $T_{f,out}$<150°C)

5. Conclusion

In this paper, a gas-solid-liquid coupled heat transfer program is developed to evaluate the flow heat transfer performance of a counter-flow tube-fin air precooler. Two methods are used to calculate the differential equation for the thermal conductivity of the precooler wall, the "Node Current Method" and the "Fenics Finite Element Platform". The following conclusions can be drawn:

(1) The calculation results of two wall temperature iteration methods, "Node Current Method" and "Fenics Finite Element Platform", using hydrogen and methane as coolants are compared. The result shows that the relative error of calculated air outlet temperatures is less than 1.1% for two methods. The accuracy of the program calculation results can also be verified by the comparison of the two methods. Kerosene with cracking mechanism can also be calculated by the program.

(2) The counter-flow tube-fin air precooler effectively handles cooling tasks for air with Mach numbers ranging from 2.5 to 6.5, corresponding to temperatures between 486 K and 1800 K. The program accurately assesses heat transfer efficiency, making it a versatile tool for evaluating various configurations of air precooler designs.

References

[1] Bulman, M. J., Siebenhaar, A.: Combined Cycle Propulsion: Aerojet Innovations for Practical Hypersonic Vehicles. 17th AIAA International Space Planes and Hypersonic Systems and Technologies Conference, San Francisco (2011)

[2] Wei, Y.: Major technological issues of aerospace vehicle with combined-cycle propulsion. Aerosp. Technol. 1, 1-12 (2022)

[3] Zou, Z. P., Wang, Y. F., Eri, Q. T., et al.: Research progress on hypersonic precooled airbreathing engine technology. Aeroengine. 47, 8-21 (2021)

[4] Zhu, D. M., Chen, M., Tang, H. L., et al.: "Over-under" concept hypersonic turbo-ramjet combined propulsion system. J. Beijing Univ. Aeronaut. Astronaut. 32, 263-266 (2006)

[5] Murray, J. J., Guha, A., Bond, A.: Overview of the Development of Heat Exchangers for Use in Air-Breathing Propulsion Pre-Coolers. Acta Astronaut., 41(11): 723-729 (1997)

[6] Harada, K., Tanatsugu, N., Sato T.: Development Study of a Precooler for the Air-Turboramjet Expander-Cycle Engine[J]. J. Propul. Power, 17(6): 1233-1238 (2001)

[7] Varvill, R.: Heat Exchanger Development at Reaction Engines Ltd. IAC-08-C4.5.2 (2008)

[8] Wang, X. Z., Zhang T. C., Lu Y., etal: An iterative analysis and design method for study of coupling processes of combustion and heat transfer in actively-cooled scramjet combustor. J J. Propul. Technol., 35(2): 213-219 (2014)

[9] Valen-Sendstad, K., Steinman, D. A.: CFD Challenge: Solutions Using a Finite Element Method Flow Solver Implemented in FeniCS. ASME 2012 Summer Bioengineering Conference, Puerto Rico (2012)

[10] Li, H., Ru, Z. L., Zou, Z. P., et al.: Investigation on Heat Transfer Characteristic of Supercritical Methane in a Microtube. J. Nanjing Univ. Aeronaut. Astronaut. 53, 513-520 (2021)